I-6359

MASTER

USE OF THE STELLARATOR EXPANSION TO INVESTIGATE
PLASMA EQUILIBRIUM IN MODULAR STELLARATORS

By

G. Anania, J.L. Johnson, and K.E. Weimer

NOVEMBER 1982

PLASMA PHYSICS LABORATORY

DISTRIBUTION OF THIS DOCUMENT IS UNLIMITED

PRINCETON UNIVERSITY
PRINCETON, NEW JERSEY

*PAGES	NTIS Selling Price	
1-25	$5.00	For documents over 600
26-50	$6.50	pages, add $1.50 for each
51-75	$8.00	additional 25 page increment.
76-100	$9.50	
101-125	$11.00	
126-150	$12.50	
151-175	$14.00	
176-200	$15.50	
201-225	$17.00	
226-250	$18.50	
251-275	$20.00	
276-300	$21.50	
301-325	$23.00	
326-350	$24.50	
351-375	$26.00	
376-400	$27.50	
401-425	$29.00	
426-450	$30.50	
451-475	$32.00	
476-500	$33.50	
500-525	$35.00	
526-550	$36.50	
551-575	$38.00	
576-600	$39.50	

USE OF THE STELLARATOR EXPANSION
TO INVESTIGATE
PLASMA EQUILIBRIUM IN MODULAR STELLARATORS

G. Anania, J.L. Johnson,[a] and K.E. Weimer

ABSTRACT

A numerical code utilizing a large-aspect ratio, small-helical-distortion expansion is developed and used to investigate the effect of plasma currents on stellarator equilibrium. Application to modular stellarator configurations shows that a large rotational transform, and hence large coil deformation, is needed to achieve high-beta equilibria.

1. INTRODUCTION.

Interest in the stellarator concept for containment of a thermonuclear plasma has recently been revived.[1,2] This is due to progress in solving several earlier difficulties. Experimental results with current-free operation of WENDELSTEIN VII-A[3] and HELIOTRON E[4] have demonstrated containment comparable with, or better than, that achieved in equivalent tokamaks. Transport studies using Monte Carlo techniques[5−7] have indicated that losses of particles trapped in non-axisymmetric magnetic fields may be less severe than previously estimated. The development of modular coils[8−11] has eliminated the problem of interconnected windings[1] which arises in classical stellarator configurations and simplified the design problems for the supporting structure. Reactor studies using conservative physics assumptions[11] lead to a reactor design that compares well with those of other fusion devices. With this renewed interest, there is a need for techniques to investigate the effect of the plasma on the magneto-hydrodynamic equilibrium and stability properties of the stellarator configuration. This paper describes how a program to do this has been implemented and applied to study some specific equilibria.

Most of the recent theoretical studies and reactor designs have used vacuum magnetic fields and ignored the effects of plasma pressure on the configuration. Three techniques have been developed for studying the actual plasma containment. Three-dimensional codes[12,13] can be used to investigate the equilibrium properties of these systems. Present computer technology is barely able to cope with these problems, so studies are restricted to relatively coarse meshes and require considerable time and effort. Furthermore, in the present codes, the shape of an outer flux surface, rather than the actual coil configuration, is usually specified. A second approach, expansion about the magnetic axis,[14−16] has provided considerable insight. This also suffers from having the surface shapes defined, as opposed to specifying the fields or currents outside the plasma. The third approach is to use the fact that stellarators are envisioned to operate with a large aspect ratio so that we can employ the stellarator expansion.[17,18] This technique is based on the assumption that the non-axisymmetric part of the

magnetic field is small and periodic over a length that is much shorter than the major radius of the system. Straightforward expansion provides an averaging over these ripples and, in lowest order, reduces the problem to an axisymmetric one. This expansion simplifies both the equilibrium and stability problems,[19] making possible the identification of the physical issues. A time-dependent code[20] based on this stellarator-expansion ordering has provided information on some special cases. Even this code uses a fixed, prescribed plasma surface as a boundary condition.

Since the equilibrium and stability equations obtained from the stellarator expansion have only minor mathematical differences from those for an axisymmetric tokamak, it is useful to modify the PEST equilibrium and stability codes[21,22] to treat these problems. We present the formulation of the equilibrium code in the next section. The approach is similar to that used in an earlier attempt.[23] Its validation is described in Sec. III. We apply the code to stellarators with modular coils in Sec. IV and provide a short discussion of the results in Sec. V.

II. FORMALISM.

The stellarator model[18] was developed to reduce the three-dimensional stellarator problem to a two-dimensional one. In this model the helical magnetic field is considered to be much smaller than the toroidal field, with a short enough wave length that its effects can be incorporated into the model by an averaging technique. We consider a magnetic field of the form

$$\mathbf{B} = \mathbf{B}_0 + (\mathbf{B}_\delta) + (\mathbf{B}_\kappa + \mathbf{B}_\beta + \mathbf{B}_\sigma + \mathbf{B}_{\delta\delta}) + ... \tag{1}$$

with an ordering in the square root of the inverse aspect ratio,

$$(\frac{B_\delta}{B_0})^2 \sim \frac{B_\kappa}{B_0} \sim \frac{B_\beta}{B_0} \sim \frac{B_\sigma}{B_0} \sim \frac{B_{\delta\delta}}{B_0} \sim \frac{a}{R} \ll 1. \tag{2}$$

We use an orthogonal (r, θ, ς) coordinate system where the metric elements are

$$h_1 = 1, \quad h_2 = r, \quad h_3 = (1 + \frac{r}{R} \cos \theta). \tag{3}$$

Here R is the major radius of the torus and r measures the distance out from the axis, with $r \approx a$ a measure of the plasma radius.

The lowest-order field $\mathbf{B}_0$ is uniform and in the ς-direction. In first order,

$$\mathbf{B}_\delta = \nabla \sum_{l,h} \frac{B_0 \epsilon_{l,h}}{h} I_l(hr) \sin(l\theta - h\varsigma) \tag{4}$$

is a vacuum field associated with current in helical coils, with l and h the multiplicity and wave number of the $\epsilon_{l,h}$ harmonic (we assume that $ha \approx 1$ with hR an integral number). The lowest-order effects of toroidal curvature, plasma pressure, and currents along the magnetic field, inside or outside the plasma, are given by

$$\mathbf{B}_\kappa = -\mathbf{e}_\varsigma B_0 \frac{r}{R} \cos\theta, \tag{5}$$

$$\mathbf{B}_\beta = -\mathbf{e}_\varsigma 4\pi p(\Psi)/B_0, \tag{6}$$

$$\mathbf{B}_\sigma = \nabla\varsigma \times \nabla A(r,\theta), \tag{7}$$

respectively, with Ψ defining a magnetic surface. These, together with a higher-order, ς-dependent vacuum field $\mathbf{B}_{\delta\delta}$, are second order, as is the inverse aspect ratio.

Solving the equilibrium equations, order by order, reduces the problem to[18]

$$\Psi = \Psi_0 - \frac{1}{B_0}\left(\int d\varsigma \mathbf{B}_\delta\right) \cdot \nabla\Psi_0 + \overline{\Psi_1}(r,\theta) + \ldots \quad, \tag{8}$$

$$\Psi_0 = \Psi_V(r,\theta) + 2\pi RA, \tag{9}$$

$$\nabla^2 A = 4\pi J_\sigma = -8\pi^2 R p'(\Psi_0)\Omega(r,\theta) + G(\Psi_0). \tag{10}$$

Here Ψ_0 is the poloidal flux,

$$\Psi_V \equiv \frac{2\pi R}{B_0} < B_{\delta r} \int B_{\delta\theta} d\varsigma >$$

$$= \pi R B_0 \sum_{l,m,h} \frac{\epsilon_{l,h}\epsilon_{m,h} m I'_l(hr) I_m(hr)}{h^2 r} \cos(l-m)\theta \tag{11}$$

measures the contribution of the vacuum multipolar fields to the magnetic surfaces, and

$$\Omega \equiv \frac{<\mathbf{B}_\delta^2>}{B_0^2} + \frac{2r}{R}\cos\theta$$

$$= \sum_{l,m,h} \frac{\epsilon_{l,h}\epsilon_{m,h}}{2}\left(I_l'(hr)I_m'(hr) + (\frac{lm}{h^2r^2} + 1)I_l(hr)I_m(hr)\right)\cos(l-m)\theta + \frac{2r}{R}\cos\theta$$

(12)

represents the effective magnetic field line curvature. The angular brackets represent an average over ς, and primes denote derivatives with respect to the argument. The function $G(\Psi_0)$ in Eq. (10), introduced as an arbitrary constant of integration in the formulation, provides the freedom to prescribe the net toroidal current on each magnetic surface. Thus it is often convenient to set

$$G(\Psi_0) = 8\pi^2 Rp'(\Psi_0)\oint \Omega(r,\theta)\frac{ds}{|\nabla\Psi_0|}/\oint \frac{ds}{|\nabla\Psi_0|} + \overline{G}(\Psi_0),$$

(13)

with $ds^2 \equiv dr^2 + r^2 d\theta^2$ on a constant-Ψ_0 cross section. The surface integral removes the net contribution to J_σ arising from the pressure term so that $\overline{G}(\Psi_0)$, which measures the ohmic heating current, is zero for a net-current-free stellarator. It is useful to note that the equilibrium properties have been determined only to lowest order, but additional information about the shapes of the surfaces is available in the second term of Eq. (8). Evaluation of $\overline{\Psi}_1(r,\theta)$ requires knowledge of the magnetic fields through third order. For many configurations it is possible to show that this term is a function of Ψ_0 alone. In this paper we adjust it so that the fluxes as calculated in first order are nearly the same when evaluated at different cross sections, and the same as obtained from the zeroth order. The change in shape of the ς-dependent part of the surfaces can be quite large, due to the fact that the gradients of Ψ_0 need not be small.

Other quantities which are useful for equilibrium and stability considerations can be evaluated by integrating around constant-Ψ_0 contours as in Eq.(13).[18] These include the rotational transform,

$$\iota \equiv \frac{d\Psi_0}{d\Phi} = (B_0\oint \frac{ds}{|\nabla\Psi_0|})^{-1},$$

(14)

and the rate of change of surface volume with toroidal flux Φ,

$$V'(\Phi) = \frac{2\pi R}{B_0}(1 + sS'(\Psi_0)) \quad , \tag{15}$$

with

$$S'(\Psi_0) \equiv B_0 \oint [\Omega(r,\theta) + \frac{4\pi}{B_0^2}p(\Psi_0)]\frac{ds}{|\nabla\Psi_0|}. \tag{16}$$

We omit the second term in Eq ?) for the purpose of investigating localized instabilities since it represents the magnetic well dug by the diamagnetic current, which can be carried along by an interchange and therefore does not contribute any stabilization.[17,24] A negative value of $V''_{vac}(\Phi)$ is favorable for suppression of these modes.

Equations (8) through (12) are very similar to the Grad-Shafranov equation which determines axisymmetric equilibrium,[21]

$$\nabla^{\bullet}\Psi \equiv X\frac{\partial}{\partial X}\frac{1}{X}\frac{\partial\Psi}{\partial X} + \frac{\partial^2\Psi}{\partial Z^2} = -4\pi^2 p'(\Psi)X^2 - 4\pi^2 R^2 B_0^2 g(\Psi)g'(\Psi), \tag{17}$$

where $RB_0 g(\Psi)\nabla\phi$ is the toroidal magnetic field and $X = R + r\cos\theta$. The differences are: (1) inclusion of the multipolar field contribution Ψ_V in the flux function, (2)modification of the curvature term Ω to include the effect of the multipolar field, and (3) use of the cylindrical Laplacian operator ∇^2 rather than the toroidal one $\nabla^{\bullet}$ because of the large-aspect-ratio expansion. We have modified the PEST equilibrium code to incorporate these changes. Evaluation of the surface integrals in Eqs. (13) through (16) is accomplished through integrations using the built-in mapping routine.

III. CODE VALIDATION.

We have tested the code's accuracy by two methods. Both show that the results agree reasonably well with those obtained using other techniques.

The first method used for code validation involves comparison with an exact quadrature solution[18] for the special case where $p(\Psi_0)$ and $G(\Psi_0)$ are linear functions of Ψ_0 so that Eq. (10) is linear. Two problems are encountered in

making this comparison. First, this special choice leads to an abrupt jump in the toroidal current at the plasma boundary so that the finite-difference inversion techniques used to solve the Poisson equation in the PEST code become inadequate. Second, evaluation of the quadrature solution becomes difficult at high β, where the surfaces are far from circular. The comparisons given in Table 1 show the agreement that could be expected when we estimate the effect of these difficulties. Further confidence can be gained from the comparison of the magnetic axis shift with increasing $\beta \equiv 8\pi p(0)/B_0^2$ shown in Fig. 1.

In the second method we compare the shift of the magnetic axis with respect to the plasma boundary as a function of beta with that obtained from other work. We find good agreement with an initial-value code[20] which utilizes the same expansion for a model with the parameters chosen to represent the WENDELSTEIN VII-A device. Comparison of the axis shift in HELIOTRON E with calculations using a fully three-dimensional code also shows agreement.[25]

IV. APPLICATION TO MODULAR STELLARATORS.

In this section we use the code to investigate the properties of modular-coil stellarator configurations.[8,9] We do this by utilizing Fourier decomposition of the current in the coils, followed by the application of the stellarator expansion. It has been shown[8] that, for large-aspect-ratio configurations, good agreement is obtained between the results of this approach and calculations of rotational transforms obtained by following magnetic field lines for vacuum-field systems. Although the agreement can not be expected to be as good for the smaller aspect ratios used in this application, the information obtained from this model can provide guidance for the evaluation and comparison of the different systems.

A limit on the harmonic content present in the field is imposed by the condition that the magnetic surfaces be well behaved.[9] In our model we would expect to see the breakdown of this condition through the lack of closure of the outer first-order magnetic surfaces obtained using Eq.(8). This often occurs because $\nabla \Psi_0$ can be very large where the zeroth-order surfaces are close to

each other. We have compared our estimates of the maximum radius at which separatrices occur with exact calculations following magnetic field lines in several vacuum-field cases[9] and observed that the limits imposed by taking our results seriously when we keep first-order terms are too pessimistic. As remarked earlier, this is due in part to our inability to evaluate $\bar{\Psi}_1(r,\theta)$ correctly. The use of an asymptotic expansion with the small parameter of the order of one-half also creates difficulties. Thus poor magnetic surfaces with this code should be accepted as an indication that a limit is being approached but should not be considered as providing a quantitative restriction. Numerical problems occur when the magnetic surfaces get closely bunched, so that in most of this work we have restricted ourselves to very low values of $\beta \equiv 8\pi p(0)/B_0^2$, at which the shift of the magnetic axis relative to the center of the plasma surface is roughly equal to half the plasma radius. This value of β has often been taken as a figure of merit for equilibrium limits. Since the shift can be directly correlated with the rotational transform, this is probably an over-simplification.

We consider the modular coil winding law

$$\varsigma = \varsigma_i + \sum_j d_j sinj(l\theta - \theta_i), \quad r = a, \quad i = 1, 2, ..., N \tag{18}$$

with $\varsigma_i \equiv 2\pi Ri/N$, $\theta_i = 2\pi mi/N$; the d_j's represent the coil deformations, l and m are the numbers of poloidal and toroidal field periods, N is the number of coils, and a is the winding radius, which we normalize to unity. We have represented the coils by keeping three terms in the winding law, $j = 1, 2,$ and 3. This law with only one harmonic, $j = 1$, was proposed as a way to obtain a stellarator configuration with a single set of modular coils.[26] The inclusion of more terms in the winding law[8,9] introduces additional harmonic content into the magnetic field. This provides an increased rotational transform but can lead to a reduction in the plasma volume because of the appearance of helical separatrices in the first-order surfaces. In this work we add a uniform vertical field as we increase the plasma pressure to keep the center of the plasma surface fixed. If we did not do this the plasma would move into a region where the contribution to the flux from the helical windings is large so that the integrity of the first-

order surfaces would be damaged. Since our model amplifies these difficulties, this modification probably makes the results more meaningful and simplifies the comparison of cases with pressure with their vacuum-field counterparts.

We first treat the Rehker-Wobig coil[26] with $l = 2$, $m = 4$, $N = 36$, $R/a = 6.2854$, $d_1/a = 0.2$, $d_2/a = d_3/a = 0$, and the plasma radius $r_p/a = 0.4875$. This coil corresponds to the solid curve in Fig. 8 of reference 9. The vacuum field contributions to the rotational transform coming from the major harmonic modes are shown in Fig. 2(e). Most of the transform can be associated with the $\sin 2(\theta - 2\varsigma/R)$ component of the magnetic field, the "helical mode" of references 8 and 9 ; the $\sin 2(\theta + 16\varsigma/R)$ component, the "anti-helical mode," accounts for much of the rest. We assume that p varies as Ψ_0^2 and we keep zero net current on every flux surface. The zeroth-order magnetic surfaces, Figs. 2(a) and 2(b), together with cross sections keeping the first-order corrections, Figs. 2(c) and 2(d), are also given for the vacuum configuration and for a case with $\beta = 2\%$. The shift of the axis with respect to the plasma surface is $\Delta/a = 47\%$. To prevent an excessive outward shift of the plasma surface we impose a small vertical field, $B_V/B_0 = 0.0077$. The rotational transform $\iota(\Psi_0)$ and $V'(\Phi)$, given by Eqs. (14) and (15) [without the last term in Eq. (16)] , are shown in Figs. 2(f) and 2(g). As should be expected, the major effect of introducing plasma pressure is the outward shift of the magnetic surfaces due to the local field produced by the Pfirsch-Schlüter current, Eq. (10) [Fig. 2(h)]. Associated with this shift is a distortion of the Ψ_0 surfaces near the magnetic axis into an elliptic shape. In this region this increases the rotational transform and the magnetic field lines spend more time on the inside of the torus, where the magnetic curvature is favorable, changing the slope of $V'(\Phi)$ and producing a magnetic well. The fields associated with these Pfirsch-Schlüter currents are quite small at the edge of the plasma so that $\iota(\Psi_0)$ and $V'(\Phi)$ approach their vacuum field values. Since there is no net current in the system and the region where $\iota(\Psi_0)$ is the same on two flux surfaces is in a magnetic well, the double-valued behavior of $\iota(\Psi_0)$ is not necessarily bad.

As shown in the dashed curve in Fig. 8 of reference 9, the rotational

transform produced by modular coils can be increased without increasing the maximum deformation by changing $d\varsigma/d\theta$ in the winding law at the nodal points $\varsigma = \varsigma_i$. A reasonable coil configuration[9] can be modeled with $l = 2$, $m = 4$, $N = 36$, $R/a = 6.2854$, $d_1/a = 0.2128$, $d_2/a = -0.0181$, $d_3/a = 0.0128$, and $r_p/a = 0.4875$. The vacuum field contribution to $\iota(\Psi_0)$ coming from the different Fourier components is given in Fig. 3. It is clear that this more complicated deformation has an increased harmonic content. In this figure we also show the magnetic surfaces, $\iota(\Psi_0)$, and $V'(\Phi)$ for cases with $\beta = 0$ and $\beta = 2.5\%$ ($B_V/B_0 = 0.0083$), and the Pfirsch-Schlüter current. The value of the vacuum rotational transform is increased by about 15% above that of the previous coil, so that even though β is higher, the axis shift, $\Delta/a = 45\%$, is smaller. This happens because the higher transform reduces the Pfirsch-Schlüter current. It can be observed that for this configuration the distortion of the first-order, ς-dependent magnetic surfaces is larger than for the previous coil.

An even higher rotational transform can be obtained from a configuration modeled with $l = 2$, $m = 4$, $N = 36$, $R/a = 6.2854$, $d_1/a = 0.24$, $d_2/a = 0$, $d_3/a = 0.04$, and $r_p/a = 0.4875$ (the dotted curve in Fig. 8 of reference 9). The results are given in Fig. 4 for $\beta = 0$ and $\beta = 4\%$ ($B_V/B_0 = 0.01$). This coil deformation further improves the rotational transform, so that $\Delta/a = 48\%$.

A much higher rotational transform can be obtained by using coils with a larger maximum deformation. To investigate the effect of increasing the deformation from 20% to 30%, we consider a configuration with $l = 2$, $m = 4$, $N = 36$, $R/a = 6.2854$, $d_1/a = 0.3354$, $d_2/a = -0.05$, $d_3/a = 0.0354$, and $r_p/a = 0.4875$. With these parameters the rotational transform on axis is $\iota = 1.11$, so that even with $\beta = 15\%$ (corresponding to an average beta of about 5%) Δ/a is only 48%. The figures for this case are not shown. We show instead those corresponding to a case that has been treated in the literature (Fig. 4 of reference 8). Its coils have the same deformation parameters but $R = 6.6667$, $m = 6$, and $N = 48$. The higher number of field periods decreases the rotational transform on axis (now $\iota = 0.81$) but gives a little more shear. As can be seen from Fig. 5, the axis shift $\Delta/a = 49\%$, at $\beta = 8\%$ ($B_V/B_0 = 0.013$),

is reasonable. As in the other cases, we see the development of a large transform and deep well at the magnetic axi.

It is frequently argued that $l = 3$ is the obvious choice for a reactor because the vacuum magnetic surfaces possess large shear. It has been noted previously[18] that addition of even a small amount of plasma pressure drastically alters the configuration. We illustrate this by treating a system with $l = 3$, $m = 9$, $N = 36$, $R/a = 6.6667$, $d_1/a = 0.3$, $d_2/a = -0.101$, $d_3/a = 0$, and $r_p/a = 0.33$. The results, given in Fig. 6, show that even for $\beta = 0.15\%$ (with no added vertical field) the shapes of the magnetic surfaces and all the equilibrium properties have changed considerably. The axis shift is $\Delta/a = 57\%$. A reasonable conclusion to draw from this treatment is that as soon as any pressure is introduced into an $l = 3$ system, the plasma quickly shifts so that its Ψ_0 surfaces become elliptic and acquire a finite rotational transform near the axis.

As has been noted,[18] the vacuum field magnetic surfaces can be modified by the addition of a particular vertical field so that the Pfirsch-Schlüter currents are small. Then, increasing the pressure should have little effect on the magnetic configuration. A uniform external vertical field with $B_V/B_0 = 0.08$ accomplishes this for this system by making $\oint dl/B$ over a periodicity length nearly independent of poloidal angle. A β of 2% is easily obtained. Although this configuration has excellent equilibrium properties, it may not be attractive because the plasma lies on a magnetic hill instead of in a magnetic well.

V. DISCUSSION.

Interest in stellarators has generated a need for techniques to investigate equilibrium and stability of three-dimensional configurations. The existing fully three-dimensional codes are restricted in accuracy because of their coarse meshes and are expensive to run. Most of the current studies utilize only vacuum-field configurations. The stellarator expansion approach can be a useful supplementary tool. Although the ideas currently being pursued lead to parameters not well

suited to the expansion this technique can identify potential advantages and investigate problems that may arise.

The cases we have shown mainly represent configurations produced by modular coils with deformations of about 20% of their winding radius. With these parameters, the maximum value of β achievable before the shift of the magnetic axis with respect to the plasma boundary becomes appreciable is quite low. This is due to the small rotational transform generated by the coils. The rotational transform can be increased by modifying the winding law to introduce more harmonics in the magnetic field. Unless care is taken, this produces surface breakup thereby effectively reducing the plasma radius. Increasing the magnitude of the deformation increases the externally imposed rotational transform and thus improves the equilibrium properties. Since the values of the expansion parameters used in this study are large, the β-limits obtained from the model are lower than what should actually be obtained. Nevertheless, it must be concluded from these results that the design of a modular device will be difficult because plasma effects quickly become important.

Our treatment of $l = 3$ configurations should serve as a warning against using the vacuum configuration for system studies when there is no rotational transform at the axis in the vacuum magnetic field. Extremely small pressure can alter the equilibrium properties dramatically.

It has been emphasized recently[27−28] that stellarators with moderate aspect ratio can have adequate rotational transforms, so the equilibrium limitations on beta due to the shifting of the magnetic surfaces are not stringent. At the same time, stability can be expected because of the favorable magnetic well created by this shift. However, most of the stellarator stability work that has been done has either treated localized interchange and ballooning modes, ignoring the effect of the force-free current, or considered tokamak-like operation with a net current but assuming concentric, circular, lowest-order magnetic surfaces without pressure, to investigate kink modes. A PEST-type stability code to complement this equilibrium code has been constructed.[29] It will allow the study of the interaction of the forces associated with the Pfirsch-Schlüter current and

those related to pressure-driven interchanges and ballocning, to obtain a better
understanding of the stability properties of stellarators.

ACKNOWLEDGMENTS

References

[a] On loan from Westinghouse Research and Development Center.

[1] W.F.Dove, G.Grieger, J.L.Johnson, D.J.Lees, P.A Politzer, J.L.Shobet, and H.Wobig, *Report of the Joint U.S.-Euratom Stellarator Steering Committee, Max-Planck Institüt für Plasmaphysik* Report IPP2/254 (July 1981) .

[2] J.L. Johnson, *Nuclear Technology / Fusion* 2, 340 (1982).

[3] D.V.Bartlett, G. Cannick, G. Cattanei, D. Dorst, G. Grieger, H.H. Hacker, J. How, H. Jäckel, R. Jaenicke, P. Javel, J. Junker, M. Kick, R. Lathe, J. Meyer, C. Mahn, S. Marlier, G. Müller, W. Ohlendorf, F. Rau, H. Renner, H. Ringler, J. Sapper, P. Smeulders, M. Tutter, B. Ulrich, A. Weller, E. Würsching, H. Wobig, M. Zippe, D. Cooper, K. Freudenberger, G. Lister, W. Ott, and E. Speth, *Plasma Physics and Controlled Nuclear Fusion Research, 1980* (International Atomic Energy Agency, Vienna, 1981), vol. 1, p. 185.

[4] A. Iiyoshi, M. Sato, O. Motojima, T. Mutoh, S. Sudo, M. Iima, S. Kinoshita, H. Kaneko, H. Zushi, S. Besshou, K. Kondo, T. Mizuuchi, S. Morimoto, and K. Uo, *Phys. Rev. Lett.* 48, 745 (1982).

[5] R.E. Potok, P.A. Politzer, and L.M. Lidsky, *Phys. Rev. Lett.* 45, 1328 (1980).

[6] A.H. Boozer and G. Kuo-Petravic, *Phys. Fluids* 24, p. 851 (1981).

[7] H.E. Mynick, T.K. Chu, and A.H. Boozer, *Phys. Rev. Lett.* 48, 322 (1982).

[8] T.K. Chu, H.P. Furth, J.L. Johnson, C. Ludeccher, and K.E. Weimer, *IEEE Transactions on Plasma Science* PS-9, 228 (1981).

[9] T.K. Chu, H.P. Furth, J.L. Johnson, C. Ludescher, and K.E. Weimer, *Nucl. Fusion* (in press).

[10] D.T. Anderson, J.A. Derr, and J.H. Shohet, *IEEE Transactions on Plasma Science* PS-9, 212 (1981).

[11] R.L. Miller and R.A. Krakowski, *Los Alamos National Scientific Laboratory Report LA-8978-MS* (August, 1981), unpublished.

[12]F. Bauer, O. Betancourt, and P. Garabedian, *A Computational Method in Plasma Physics*, Springer Series in Computational Physics (Springer-Verlag, New York, 1978).

[3]R.Chodura and A.Schlüter, *J. Comput. Phys.* **41**, 681 (1981).

[14]C. Mercier, *Nucl. Fusion* **4**, 213 (1964).

[15]L.S.Solov'ev and V.D.Shafranov, *Reviews of Plasma Physics*, M.A. Leontovich, ed. (Consultants Bureau, New York, 1970), vol. 5, p. 1.

[16]D.Lortz and J.Nührenberg, *Z. Naturforsch.* **34a**, 167 (1979).

[17]J.L.Johnson, C.R.Oberman, R.M.Kulsrud, and E.A.Frieman, *Phys. Fluids* **1**, 281 (1958).

[18]J.M.Greene and J.L.Johnson, *Phys. Fluids* **4**, 875 (1961).

[19]J.L.Johnson, *Max-Planck Institut für Plasmaphysik* Report 3/162 (August 1977), unpublished.

[20]H.R.Strauss and D.A.Monticello, *Phys. Fluids* **24**, 1148 (1981).

[21]J.L. Johnson, H.E. Dalhed, J.M. G.eene, R.C. Grimm, Y.Y. Hsieh, S.C. Jardin, J. Manickam, M. Okabayashi, R.G. Storer, A.M.M. Todd, D.E. Voss, and K.E. Weimer, *J. Comput. Phys.* **32**, 212 (1979).

[22]R.C. Grimm, J.M. Greene, and J.L. Johnson, *Methods in Computational Physics*, J. Killeen, Ed. (Academic Press, New York, 1976), vol. 16, p. 253.

[23]D. Elkin, T.F. Yang, and J.L. Johnson, *Bull. Am. Phys. Soc.* , vol 24, 110 (1979).

[24]J.M. Greene and J.L. Johnson, *Advances in Theoretical Physics*, K. Brueckner, ed. (Academic Press, New York, 1965), vol. 1, p. 195.

[25]G. Anania, R.C. Grimm, D. Ho, J.L. Johnson, R.M. Kulsrud, J. Manickam, K.E. Weimer, G. Berge, W.H. Choe, J.P. Freidberg, P.A. Politzer, P. Rosenau, D. Sherwell, O. Betancourt, M. Mond, and H. Weitzner, *Plasma Physics and Controlled Nuclear Fusion Research* , 1982 (International Atomic Energy Agency, Vienna, 1983) Baltimore Conf. Paper IAEA-CN41/v10.

[26] S. Rehker and H. Wobig, *Proc. Seventh Symposium on Fusion Technology*, Grenoble (October 1972) Euratom Report EUR 4938e, p. 345.

[27] L.M. Kovrizhnykh and S.V. Shchepetov, *Fiz. Plazmy* **7**, 965 (1981) [Sov. J. Plasma Phys. **7**, 527 (1981)] .

[28] M.I. Mikhailov and V.D. Shafranov, *Plasma Phys.* **24**, 233 (1982).

[29] G. Anania and J.L. Johnson, *Bull. Am. Phys. Soc.* **27** (October, 1982) .

Table 1. Comparison of the stream function $A(r, \theta)$, given at equal intervals of $\Delta x = 0.0103$ across the horizontal midplane of the plasma, inside to outside, as calculated by the quadrature formula Eq. 68 of Ref. 18 and by the code. The parameters are $l = 3$, $\beta = 2.5\%$, $R = 1$, $a = 0.062$, $\epsilon^2 = 10$, $ha = 1.24$, $G(\Psi) = G_0 + G_1\Psi$, with $G_1 = -0.005$ and $G_0 = -0.0138$, adjusted to give zero net total current.

Analytical (10^{-4})	Computational (10^{-4})	% difference
-1.306	-1.345	-2.98
-1.692	-1.717	-1.46
-1.863	-1.871	-0.42
-1.753	-1.750	0.17
-1.371	-1.384	0.48
-0.785	-0.781	0.59
0.000	0.000	0.00
0.857	0.854	-0.44
1.738	1.735	-0.20
2.569	2.574	0.19
3.261	3.287	0.79
3.688	3.757	1.87
3.646	3.806	4.40

Fig. 1. Shift of the magnetic axis with respect to the center of the plasma boundary for the $l = 3$ stellarator of Table 1, with $G_1 = -\beta/5$ and G_0 adjusted to give zero net total current. The solid curve is the result of the quadrature model of Ref. 13, while the crosses are the results obtained by the code.

Fig. 2. Equilibrium properties of a modular stellarator configuration with $l = 2$, $m = 4$, $N = 36$, $R/a = 6.2854$, $d_1/a = 0.2$, $d_2/a = 0$, $d_3/a = 0$, and $r/a = 0.4875$, giving $\iota_{vac}(0) = 0.385$. (a) Zeroth-order magnetic surfaces with $\beta = 0$. (b) Zeroth-order magnetic surfaces with $\beta = 2\%$. (c,d) Magnetic surfaces, keeping first-order terms, for $\beta = 2\%$ at $\phi = 0°$ and $\phi = 22.5°$. (e) Contribution to the vacuum rotational transform from the different field harmonics: long-dashed curves, helical mode $\sin 2(\theta - 2\varsigma/R)$ (upper) and $\sin 2(\theta - 20\varsigma/R)$ (lower) ; short-dashed curve, anti-helical mode $\sin 2(\theta + 16\varsigma/R)$; solid curve, total transform. (f) Rotational transform: dashed curve, $\beta = 0$; solid curve, $\beta = 2\%$. (g) $V'_{vac}(\Phi)$: dashed curve, $\beta = 0$; solid curve, $\beta = 2\%$. (h) Toroidal current along the horizontal midplane, $\theta = 0$ and π.

Fig. 3. Equilibrium properties of a modular stellarator configuration with $l = 2$, $m = 4$, $N = 36$, $R/a = 6.2854$, $d_1/a = 0.2128$, $d_2/a = -0.0181$, $d_3/a = 0.0128$, and $r/a = 0.4875$, giving $\iota_{vac}(0) = 0.441$. The curves are the same as in Fig. 2. but with $\beta = 2.5\%$.

Fig. 4. Equilibrium properties of a modular stellarator configuration with $l = 2$, $m = 4$, $N = 36$, $R/a = 6.2854$, $d_1/a = 0.24$, $d_2/a = 0$, $d_3/a = 0.04$, and $r/a = 0.4875$, giving $\iota_{vac}(0) = 0.554$. The curves are the same as in Fig. 2, but with $\beta = 4\%$. Since the contributions from the different helical components to the rotational transform were given in Fig. 9 of Ref. 9, a contour plot of the Pfirsch-Schlüter current is given in (e).

Fig. 5. Equilibrium properties of a modular stellarator configuration with $l = 2$, $m = 6$, $N = 48$, $R/a = 6.6667$, $d_1/a = 0.3354$, $d_2/a = -0.05$, $d_3/a = 0.0354$, and $r/a = 0.4875$, giving $\iota_{vac}(0) = 0.816$. The curves are the same as in Fig. 2, but with $\beta = 8\%$ ($\phi = 0°, 15°$) . In (e) the long-dashed curves are the helical modes $\sin 2(\theta - 3\varsigma/R)$ (upper) and $\sin 2(\theta - 27\varsigma/R)$ (lower), and the short-dashed curve is the anti-helical mode, $\sin 2(\theta + 21\varsigma/R)$

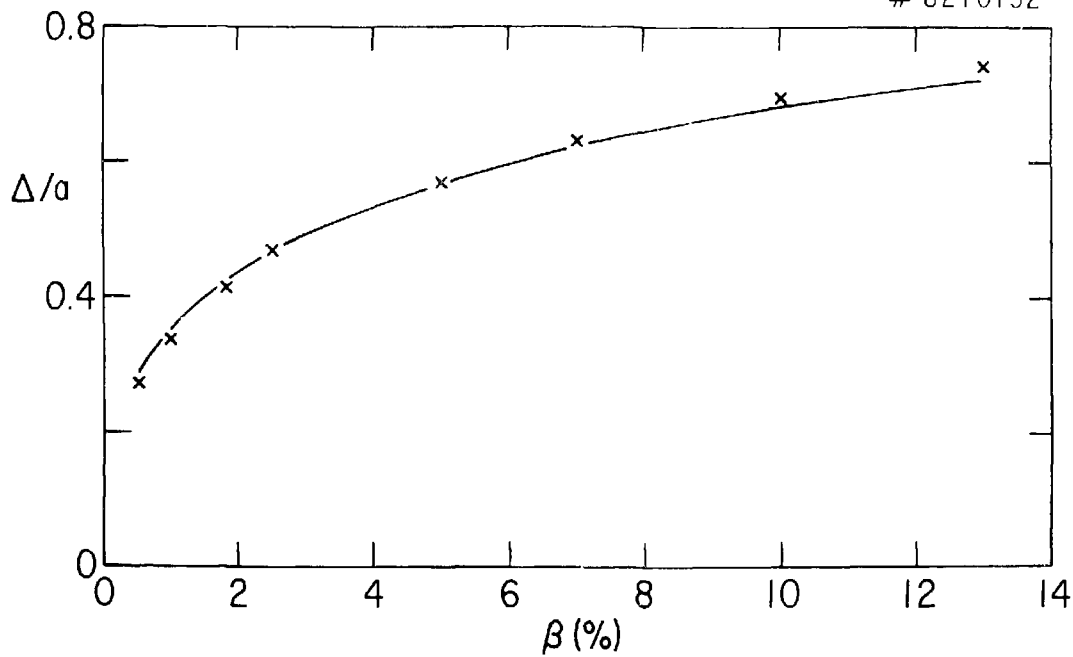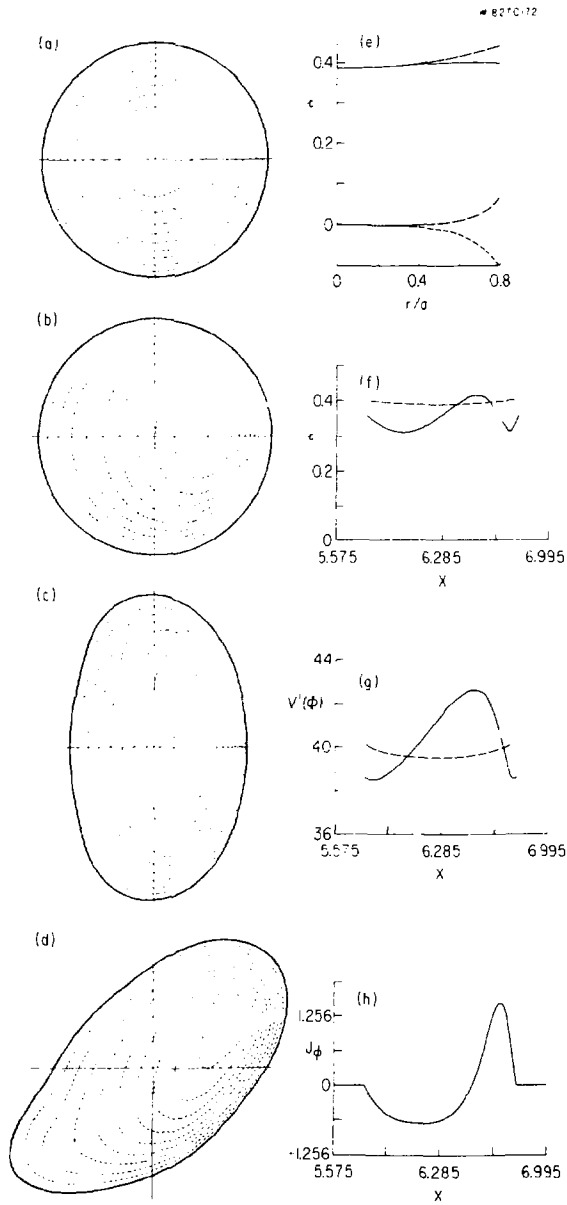Fig. 6. Equilibrium properties of a modular stellarator configuration with $l = 3$, $m = 9$, $N = 36$, $R/a = 8.6667$, $d_1/a = 0.3$, $d_2/a = -0.101$, $d_3/a = 0$, and $r/a = 0.33$. The curves are the same as in Fig. 2, but with $\beta = 0.15\%$ ($\phi = 20°, 10°$). In (e) the long-dashed curves are the helical modes $\sin 2(\theta - 3\varsigma/R)$ (upper) and $\sin 2(\theta - 15\varsigma/R)$ (lower), and the short-dashed curve is the anti-helical mode, $\sin 2(\theta + 9\varsigma/R)$
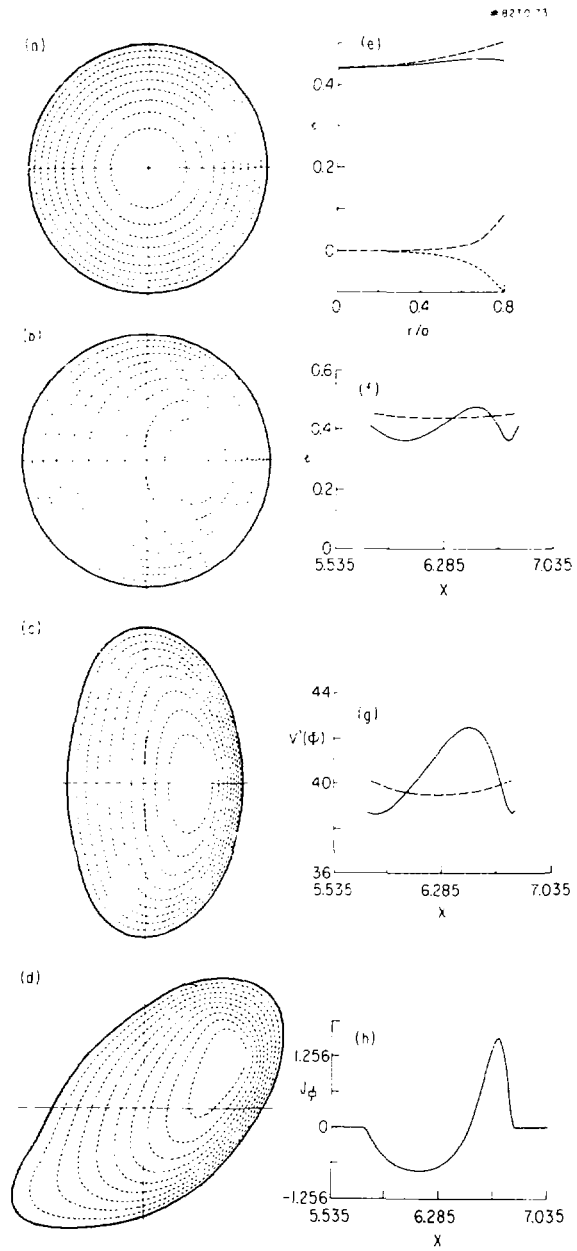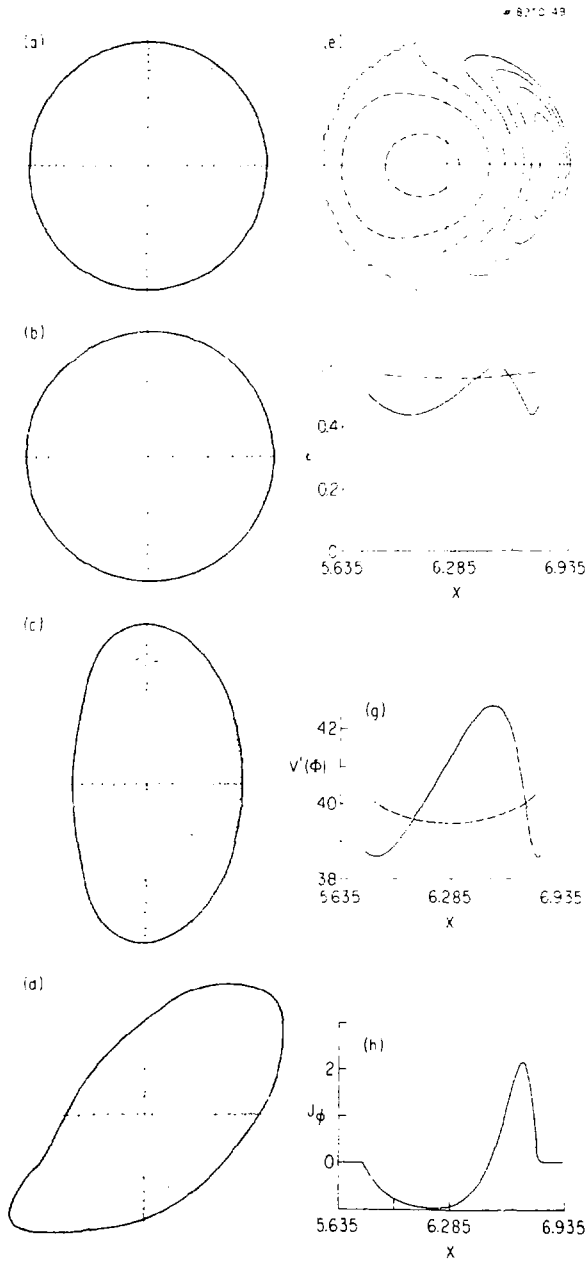
82T0152

Fig. 1

Fig. 2

Fig. 3

Fig. 4

Fig. 5

Fig. 6